

ORIGINAL PAPER

Morphology and Ultrastructure of Multiple Life Cycle Stages of the Photosynthetic Relative of Apicomplexa, *Chromera velia*

Miroslav Oborník^{a,1}, Marie Vancová^{a,1}, De-Hua Lai^a, Jan Janouškovec^b,
Patrick J. Keeling^b, and Julius Lukeš^{a,2}

^aBiology Centre, Institute of Parasitology, Czech Academy of Sciences, and Faculty of Science,
University of South Bohemia, 37005 České Budějovice (Budweis), Czech Republic

^bDepartment of Botany, University of British Columbia, Vancouver, V6T 1Z4, Canada

Submitted November 27, 2009; Accepted February 7, 2010
Monitoring Editor: B. S. C. Leadbeater

Chromera velia is a photosynthetic alga with a secondary plastid that represents the closest known photosynthetic relative of the apicomplexan parasites. The original description of this organism was based on brownish, immotile coccoid cells, which is the predominating stage of *C. velia* in the culture. Here we provide a detailed light and electron microscopy description of coccoid cells of *C. velia* and a previously undocumented bi-flagellated stage that is highly motile and moves in a characteristic zig-zag pattern. Transformation from a coccoid into a flagellate stage occurs in exponentially growing cultures, and is accelerated by exposure to light. The *C. velia* cells contain a pseudoconoid, which is likely homologous to the corresponding structure in the apical complex of Apicomplexa, cortical alveoli subtended by subpellicular microtubules, mitochondrion with tubular cristae, a micropyle, and a distinctive chromerosome, an apparently novel type of extrusion organelle. Ultrastructural analysis of the flagellate supports its close association with colpodellids and apicomplexans and provides important insight into their evolution.

© 2010 Elsevier GmbH. All rights reserved.

Key words: *Chromera*; Apicomplexa; *Colpodella*; dinoflagellate; phylogeny; ultrastructure

Introduction

The discovery, more than a decade ago, of a non-photosynthetic relic plastid termed the apicoplast in apicomplexan parasites, represented a major breakthrough for our understanding of evolution of this mostly parasitic group (Köhler et al. 1997; McFadden et al. 1996). The Apicomplexa

were already known to be related to dinoflagellate algae, but this now intensely studied organelle more directly suggested a photosynthetic ancestry for the Apicomplexa, and the possibility that other photosynthetic relatives might exist. Such a relative was indeed identified in the recently described photosynthetic alveolate, *Chromera velia* (Moore et al. 2008). This species was isolated from the stony coral *Plesiastrea versipora* in Australia by procedures usually used to isolate intracellular endosymbionts of corals, such as the dinoflagellate *Symbiodinium*. Indeed, the stage isolated

¹Both authors contributed equally to this study

²Corresponding author; fax +420 385310388
e-mail jula@paru.cas.cz (J. Lukeš).

from corals was immotile, oval in shape, and brownish-green in color, superficially resembling *Symbiodinium* (Blank 1987; Muller-Parker and Davy 2001; Stat et al. 2006). However, despite the morphological similarity between *Chromera* and symbiotic dinoflagellates, phylogenetic evidence based on several nuclear and plastid genes strongly supports its close relationship to the apicomplexan parasites (Moore et al. 2008; Oborník et al. 2009; Janouškovec et al. 2010).

Several ultrastructural features of *C. velia*, such as cortical alveoli subtended by a sheet of microtubules and a micropore, also confirm its affiliation with other alveolates (Moore et al. 2008). However, the morphology of *Chromera* remains only partly investigated, including the presence or absence of a number of interesting structural features of Apicomplexa. In the original description the existence of an uncharacterized flagellate stage was noted, and we have also observed flagellates. Because it seems likely that the flagellate stage contains ultrastructural features of interest, for example homologues of some elements of the apical complex such as the conoid, we undertook a detailed light and electron microscopic study of this flagellate. We also present a description of the life cycle, with concomitant observations of its behavior under various cultivation conditions. Altogether, we have found typical apicomplexan features, shedding further light on the early evolution of the Apicomplexa.

Results

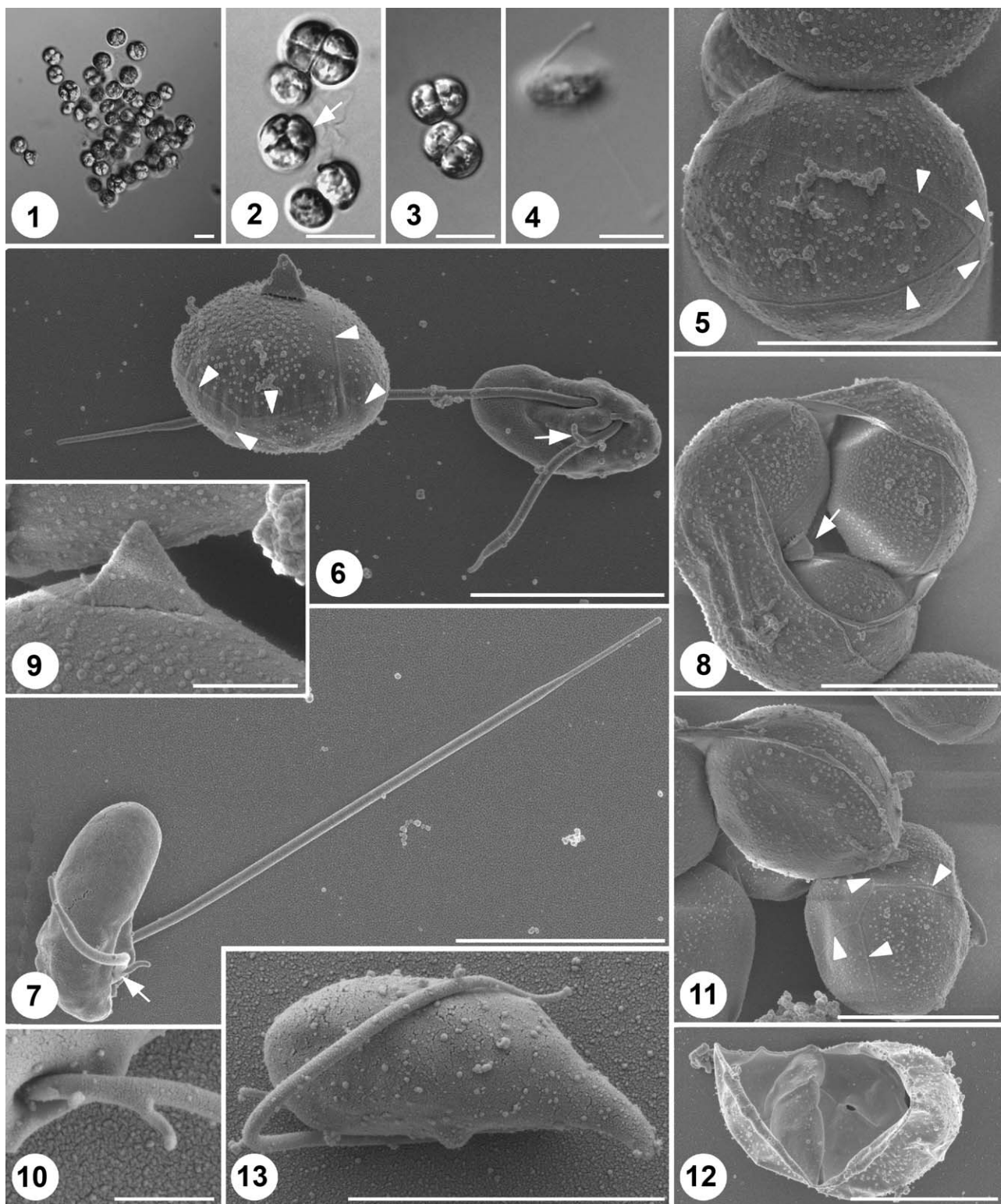
Light Microscopy

As described previously, *C. velia* can be easily grown in a simple cultivation medium (Moore et al. 2008). With the aim of establishing optimal cultivation protocol, we have experimented with cultivating

Chromera under various light conditions, in different cultivation volumes, in stationary or shaking cultivators, and using short- or long-term passages. The 12/12 hours light/dark regime with light intensity of 3.15 W m^{-2} at 26°C supported growth to the density of approximately 10^6 cells/ml. Under these conditions most cells stay at the bottom of the flask, forming a thin brownish layer. An absolute majority of these cells are immotile, round or oval brown balls and are either single or form irregular clumps (Fig. 1). However, we found that *C. velia* is able to grow at a wide range of conditions. The lower limit for its growth is 10°C and the culture flourishes at a wide range of temperatures from 22 to 31°C (O. Prášil personal commun.). The culture survived when kept for 5 days in total darkness, although under such sub-optimal conditions only cyst-like stages are present, suggesting that the culture is dormant.

In general, we distinguish three life stages, coccoid, cystic and flagellate, the prevalence of which depends on the culture growth rate (see below). The mostly oval coccoid stage is abundant in all culture conditions, and ranges in size from 5.1 to $9.5 \mu\text{m}$ (mean $7.0 \times 7.6 \mu\text{m}$) in diameter ($n=50$) (Figs 1, 2 and 57). Coccoid cells undergo binary fission resulting in two cells enclosed by a thin coccoidal wall that ranges from 7.6 to $11.2 \mu\text{m}$ long (mean $9.5 \mu\text{m}$) and 6.2 to $8.7 \mu\text{m}$ wide (mean $7.7 \mu\text{m}$) (Figs 2 and 3). Due to abundant presence of both stages in exponentially growing culture, we propose that two daughter coccoid cells are released upon rupture of the coccoidal wall and shortly afterwards commence another round of division (Fig. 57). In addition, it appears that another round of division may lead to a large cyst containing four tightly packed identical daughter cells (Fig. 3), a stage more frequently present in stationary (Fig. 1) than exponential cultures (Fig. 57). The diameter of the four-celled oval coccoid ranges from 7.9

Figures 1-13. Light (Figs 1-4) and scanning electron microscopy (Figs 5-13). **Fig. 1.** A stationary culture. **Fig. 2.** A coccoid cyst from culture containing two or four coccoids (arrow). **Fig. 3.** Two bi-cellular coccoid stages. **Fig. 4.** A motile bi-flagellated stage. **Fig. 5.** Coccoid wall with four longitudinal ridges (arrowheads). **Fig. 6.** Representatives of motile and immotile stages found in culture. The coccoid stage with inconspicuous ridges (arrowheads) and chock-like cyst residuum still attached to it lies over a flagellate. The long flagellum is tapered at its terminal part, while the short flagellum carries a finger-like projection at its basal part (arrow). Both flagella, separated by a small ridge, exit from the cell in about 90° angle from a flattened ventral side of the cell. **Fig. 7.** A flagellate with accentuated flagellar dimorphism. The tapered terminal 1/5 of the long flagellum is well visible. **Fig. 8.** A cyst with a ruptured cyst wall revealing three tightly bound coccoids and the cyst residuum (arrow). **Fig. 9.** Detail of the wedge-shaped cyst residuum. **Fig. 10.** Detail of the basal part of the short flagellum invariably carrying a finger-like projection. **Fig. 11.** A group of coccoids, with the bottom one revealing the mutual position of four longitudinal ridges (arrowheads) that are joined via a short connection. **Fig. 12.** View of an inner face of the cyst wall revealing that it does not contain any sutures. **Fig. 13.** A rare flagellate with a tapered and extended end. Scale bar = $10 \mu\text{m}$ (1-3), $5 \mu\text{m}$ (4-8,11-13) and $1 \mu\text{m}$ (9,10).



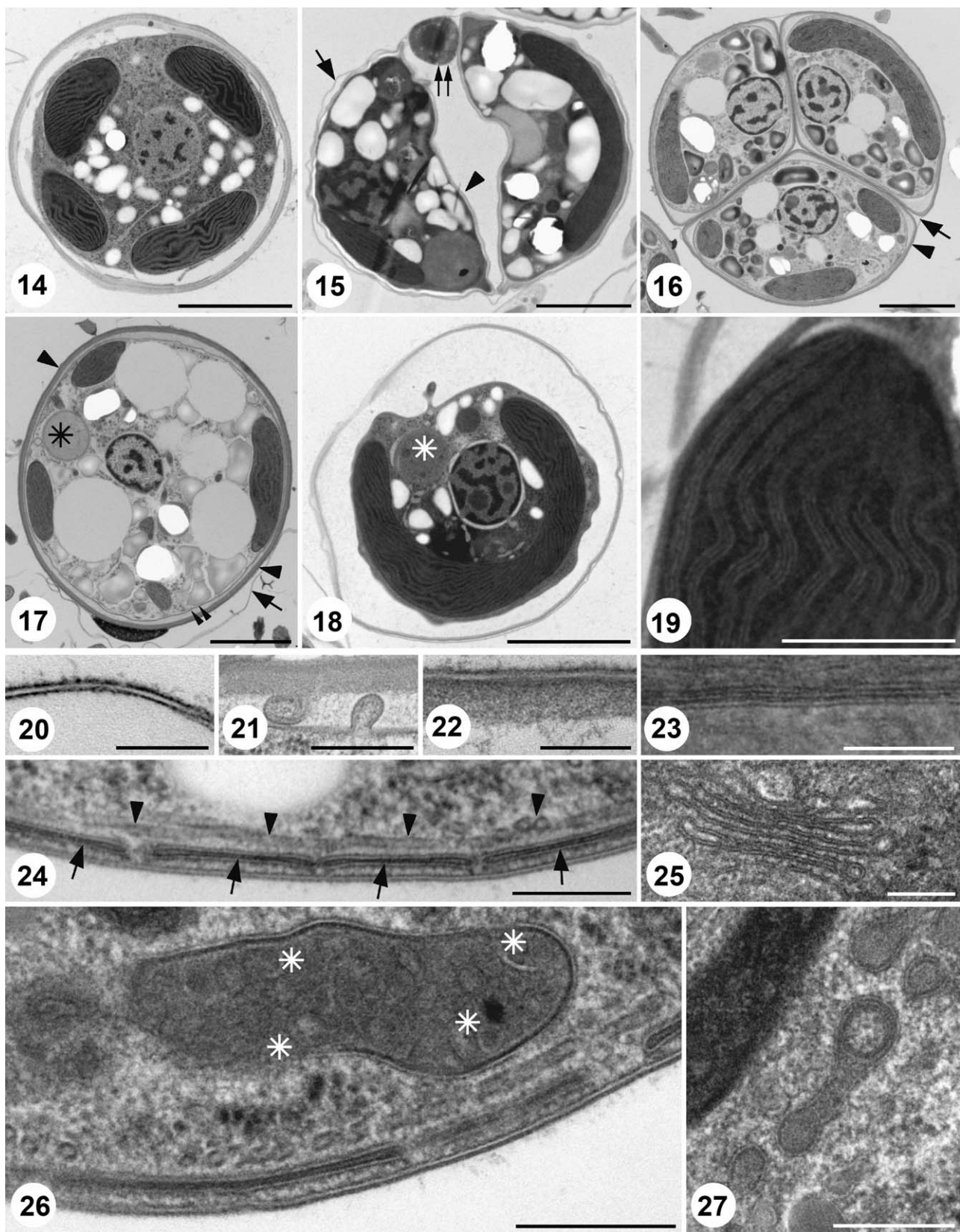
to 12.1 μm (mean 9.5 μm). Three cells are usually arranged in parallel, with the fourth one positioned perpendicularly and visible only in another focal plane (*Figs 2 arrow, and 57*). In stationary culture the cystic coccoid is the most frequent stage.

The transformation into the highly motile bi-flagellated stage (*Fig. 4*) commences with a slow spinning movement of the immotile coccoid stage, and the process takes several minutes altogether. Exflagellation occasionally occurs also in bi-cellular coccoids, but was more frequently observed in the coccoids containing four daughter cells. Regardless of light regime, transformation of coccoids into the flagellates occurs constantly in stationary culture, but in low light takes place at a very low rate, with flagellates never exceeding 1% of all cells. The emerging flagellates are elongated, with length ranging from 4.9 to 7.3 μm and width ranging from 2.7 to 4.8 μm ($n=50$). They are equipped with two heterodynamic flagella, of which only the long and conspicuous one can be observed in light microscopy (*Fig. 4*). Flagellates move at very high speed, so their distinctive movement patterns were reconstructed from video sequences (*Fig. 58*). Briefly, the cell is propelled forward in a zig-zag manner by regular beating of its posteriorly-directed flagella. The cell changes direction approximately every 250 to 375 ms as a consequence of a rotation of the cell (*Fig. 58*). After running into a clump or a higher density area, the flagellate switches into a circular movement (data not shown). In an experiment, in which freshly inoculated (=exponential) cultures kept at a 12/12 light/dark regime at 26°C were observed for a period of 14 days, we followed the (dis)appearance of the flagellates (*Fig. 60*). Although very few motile cells were observed

throughout the cultivation, exflagellation started on day 7 and the number of flagellates grew, progressively reaching a peak on day 11, after which the transformation into a motile stage slowly and steadily decreased (*Fig. 60*).

Moreover, there is a clear correlation between the emergence of the motile stages and the 24 hr light:dark cycle. As shown in Graph 2, there is a rapid transformation into flagellates 2 hrs after illumination, which peaks within another 2 hrs. Then the number drops within the following 4 hrs and then slowly but steadily abates, so that only coccoids are present in the culture 7 hrs after initial exflagellations, when the dark period starts (*Fig. 61*). Observations of motile stages individually transferred into small volumes in Elisa plates revealed that they remain motile for a maximum of 3 hrs, after which most flagellates acquire a round shape (*Fig. 59*). The transformation is rather quick and commences immediately after the motility stops. In individually followed flagellates, 35% (44 out of 126 cells) turned under our experimental conditions into the single-celled coccoids, while the remaining flagellates died. These coccoids are slightly smaller than those found in exponential culture, ranging from 4.2 to 8.2 μm in length and 5.5 to 8.3 μm (average $5.8 \times 6.8 \mu\text{m}$). They are capable of further division(s), producing either two- or four-celled coccoid cysts. Interestingly, the intensity of illumination has a dramatic effect on the percentage of cysts undergoing transformation. When the culture flasks are illuminated with 35.8 W m^{-2} , the number of motile cells increases up to ten-fold, and they appear significantly earlier (*Fig. 62*). Under these conditions exflagellation peaks on day 5. The life cycle, as we have observed it, does not seem to

Figures 14-27. Transmission electron microscopy. **Fig. 14.** Cross section of a typical coccoid, containing a single peripherally located and prolonged chloroplast, central nucleus and small amylopectin granules. **Fig. 15.** Section through a cyst containing two coccoids enclosed by a veil-like cyst wall (arrow). Note that the coccoid cell wall (arrowhead) is substantially thicker than the cyst wall. Putative cyst residuum is labeled with a double arrows. **Fig. 16.** Cross section through three tightly bound coccoids. The cyst and coccoid walls are labeled with an arrowhead and an arrow, respectively. **Fig. 17.** Cross-sectioned coccoid with amylopectin and lipid granules that occupy most of its lumen. The ruptured thin cyst wall (arrow), the thick coccoid wall (arrowhead) and the plasmalemma (double arrowhead) are well visible. **Fig. 18.** Cross-sectioned coccoid in which most of the lumen is occupied by chloroplast and nucleus. It contains very few amylopectin and lipid granules. Early putative stage of pseudoconoid (see below) is labeled with an asterisk (also in Fig. 17). **Fig. 19** Longitudinal section through a plastid with thylakoids arranged in stacks of three. **Fig. 20.** Veil-like cyst wall. **Fig. 21.** Vesicles budding off the plasmalemma. **Fig. 22.** Thick coccoid wall. The membranaceous upper layer is supported by a thicker inner layer. **Fig. 23.** Four membranes enclosing the secondary plastid. **Fig. 24.** The plasmalemma of a coccoid is underlaid by flat cortical alveoli (arrows). A single layer of subalveolar microtubules (arrowheads) lies on cytoplasmic face of the alveoli. **Fig. 25.** A prominent Golgi apparatus. **Fig. 26.** Longitudinal section through a single mitochondrion. Multiple peripherally-located tubular cristae are indicated by asterisks. **Fig. 27.** Vesicles found frequently in the cytoplasm, which are likely derived from the Golgi apparatus. Scale bar = 2 μm (14-18), 500 nm (19), 200 nm (21,24-27), and 100 nm (20,22,23).



involve sexual reproduction. Since *Chromera* was originally isolated as a symbiont of corals, the sexual part of its life cycle could eventually be hidden in its scleractinian host.

Scanning Electron Microscopy

Both stationary and exponential cultures were processed for scanning electron microscopy (SEM). As shown in Figure 8, a thin veil-like wall tightly encloses four (just three visible) coccoids within the cyst. When the cyst wall is ruptured (Fig. 8), a small, pyramidal-shaped structure is visible (Fig. 8, arrow). This is likely a sporulation residuum that either fills space not packed with the four cells, or perhaps keeps the individual coccoid cells in defined positions (Figs 6 and 9). There are four inconspicuous longitudinal ridges in the coccoid wall that come together at the poles of the coccoid cell (Fig. 5, arrowheads). Alternatively, a junction of two neighboring ridges is joined with a junction of the opposite ridges via a short connection (Fig. 11, arrowheads). A ruptured wall of the coccoid cyst is shown in Figure 12. In Figure 6, a flagellate lies next to a coccoid cell (with a pyramidal sporulation residuum still attached to its surface), the surface of which has several inconspicuous ridges (Fig. 6, arrowheads). SEM reveals that both flagella exit from an anterior part of the flattened ventral face of the smooth elongated stage (Fig. 6). The basal part of the free flagella lies in shallow longitudinal grooves separated by a short narrow ridge (Fig. 6 and data not shown). The longer flagellum, the length of which exceeds the cell by about three times, narrows significantly at its terminal portion (Fig. 7). Close to its emergence from the cell, the short flagellum invariably bears a finger-like projection about 500 nm in length (Figs 7 and 10). A

few motile cells were observed to be pointed at the anterior end and possess somewhat shorter flagella (Fig. 13, the other flagellum is not visible in this micrograph).

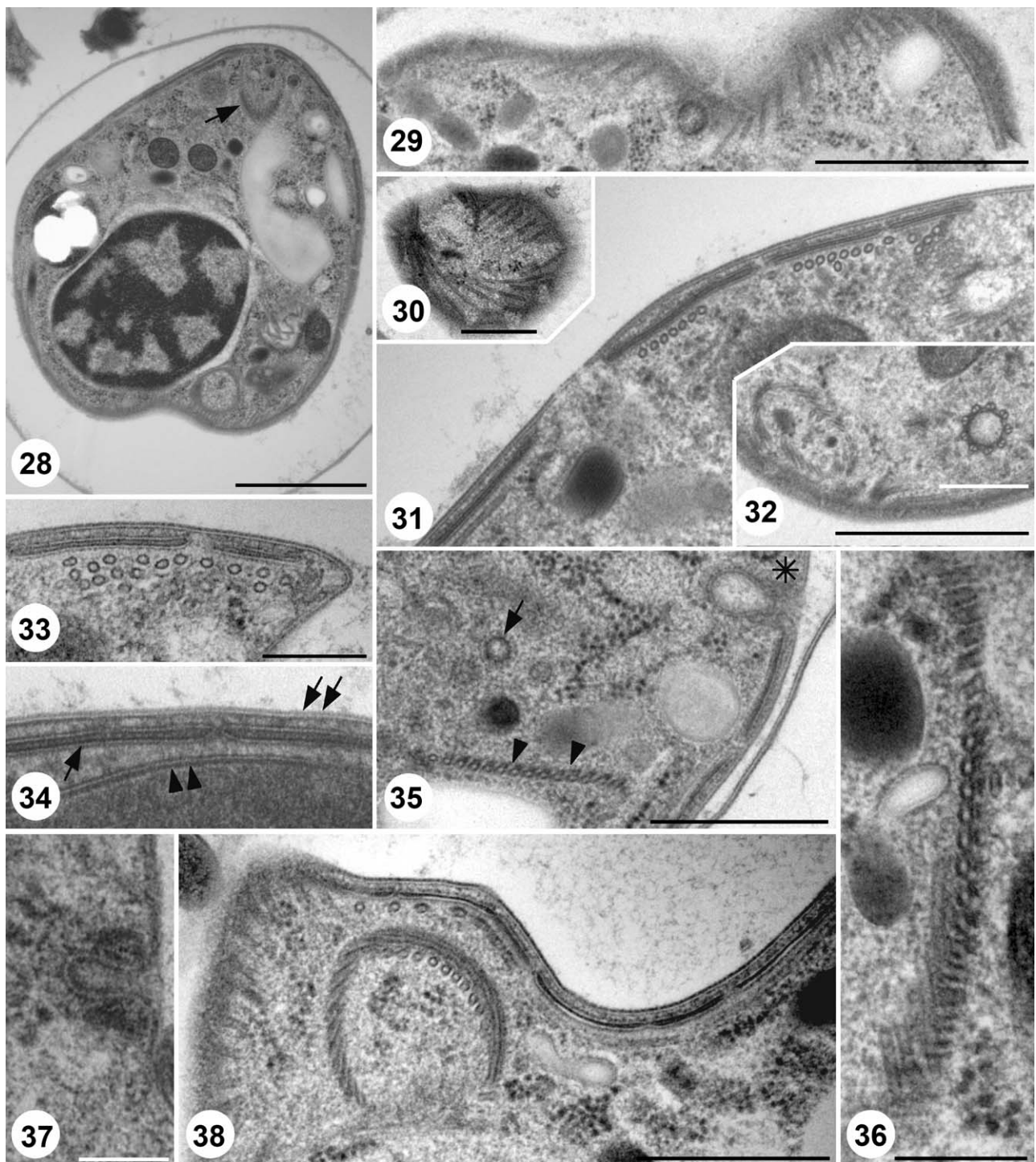
Transmission Electron Microscopy

Coccoid Stage

Preparation of the samples for TEM proved to be a challenge, most likely because of the cell walls that are resistant to penetration by fixative, as are those of coccidians. While the standard protocol resulted in poor preservation of the ultrastructural features, a breakthrough was achieved with high-pressure freezing and freeze-substitution (for details see Methods).

Cross sections of coccoid cells revealed the presence of numerous small oval granules, reminiscent of amylopectin granules of Apicomplexa, and a round nucleus containing scattered chromatin (Fig. 14). A peripherally located electron-dense plastid dominates the cell's fine structure, as it is sectioned several times due to its elongated shape (Fig. 14). Section of a bi-cellular coccoid revealed a characteristic sausage-shaped plastid in the right cell (Fig. 15). The thin cyst wall and the thick coccoid wall are indicated by arrow and arrowhead, respectively. The electron dense material located between the cells is likely a sporulation residuum (Fig. 15, double arrow). The most characteristic stage of the culture, however, is a coccoid cyst containing four tightly packed identical coccoids, with three being cross-sectioned in Figure 16. The very thin veil-like cyst wall (Fig. 20) is tightly stretched around the coccoid cells (Figs 15 and 16, arrow), which have already formed a thick wall (Figs 15 and 16, arrowhead). The cytoplasm is filled with putative amylopectin and lipid granules that are irregular in size and

Figures 28–38. Transmission electron microscopy. **Fig. 28.** An advanced pear-shaped coccoid with a microtubular root or pre-conoid in its anterior end (arrow). It is still enclosed in the cyst wall. **Fig. 29.** A corset of subalveolar microtubules. **Fig. 30.** Section through the tip of the cell revealing its complete corset of subalveolar microtubules. **Fig. 31.** Section through the periphery of the coccoid, with unevenly spaced alveoli and irregularly distributed underlying microtubules. **Fig. 32.** Anterior part of the cell containing a fan-shaped bi-layered microtubular root or pre-conoid. Subalveolar microtubules and cortical alveoli are also well visible. **Fig. 33.** Changes in the organization of subalveolar microtubules in a specific region. **Fig. 34.** Section through a peripheral region of a coccoid, in which alveoli (arrow) are not subtended by subalveolar microtubules. Double arrow and double arrowheads indicate coccoid and mitochondrial walls, respectively. **Fig. 35.** An almost straight array of microtubules (arrowheads) in the vicinity of an early micropyle, likely representing the lower part of the pseudoconoid. A clathrin-coated vesicle is marked with an arrow, while an asterisk depicts a prominent micropyle. Clusters of ribosomes are visible between both structures. **Fig. 36.** Section of the cell in which the straight array of microtubules transforms into a fan-shaped formation by gradual tilting of the microtubules. **Fig. 37.** A micropyle with its opening surrounded by electron-dense collar. **Fig. 38.** Anterior part of the cell containing a fan-shaped bi-layered pseudoconoid. Subalveolar microtubules and cortical alveoli are also well visible. Scale bar = 1 µm (28, 29, 32), 500 nm (30, 31, 35, 38), 200 nm (33, 34, 36), and 100 nm (37).



shape (Fig. 16). The coccoids in Figures 17 and 18 represent two extremes encountered in the culture. In Figure 17 the cytoplasm of a coccoid cell is virtually filled with various granules and inclusions, most likely containing storage compounds. The thick coccoid wall (arrowhead) is detached from the plasmalemma (double arrow) and adheres to the much thinner ruptured cyst wall (arrow). These cysts are more abundant in the stationary culture. In contrast, the coccoid cell in Figure 18 has very few granules, and most of the cytoplasm is occupied by the plastid and the nucleus. These cells were more common in log phase cultures.

The single dense plastid is located at the periphery of the cell and is filled with long, electron-lucent thylakoids arranged in stacks of three (Fig. 19). Each thylakoid is about 10 nm thick and runs in parallel with the axis of the elongated plastid (Figs 18 and 19). Four tightly apposed membranes (Fig. 23) testify to the secondary endosymbiotic origin of the plastid, i.e. an organelle acquired with a prey, which was most likely the primary plastid-containing alga. The thin cyst wall is composed of the inner and outer electron-dense layers and a somewhat thicker central electron-lucent layer, in total not exceeding 20 nm in diameter (Fig. 20). The thick coccoid wall appears to be assembled from small vesicles budding off the sporocyst plasmalemma (Fig. 21). It is composed of an upper layer, which has a similar structure as the cyst wall, and an inner ~ 50 nm thick layer (Fig. 22).

Just beneath the plasmalemma is a continuous layer of ribbon-shaped cortical alveoli (Fig. 24, arrows) that are typically ~ 200 nm wide and ~ 25 nm thick on average (Fig. 24). Another prominent feature of the *C. velia* sub-surface is the presence of subpellicular microtubules. As in related protists, a single layer of these longitudinally sectioned microtubules are subtended by the cortical alveoli (Figs 24, arrowheads and 26). Based on cross-sectioned tips of the cells, we estimate the total number of subpellicular microtubules to be about 25. The mitochondrion is elongated, most likely present in one copy per cell, and usually peripherally located (Fig. 26). More or less evenly distributed tubular cristae are visible within the lumen (Fig. 26, asterisks). The Golgi apparatus is typical (Fig. 25) and numerous single and apparently double membrane bounded vesicles of uncertain identity are also visible (Fig. 27).

Transformation into a Flagellate

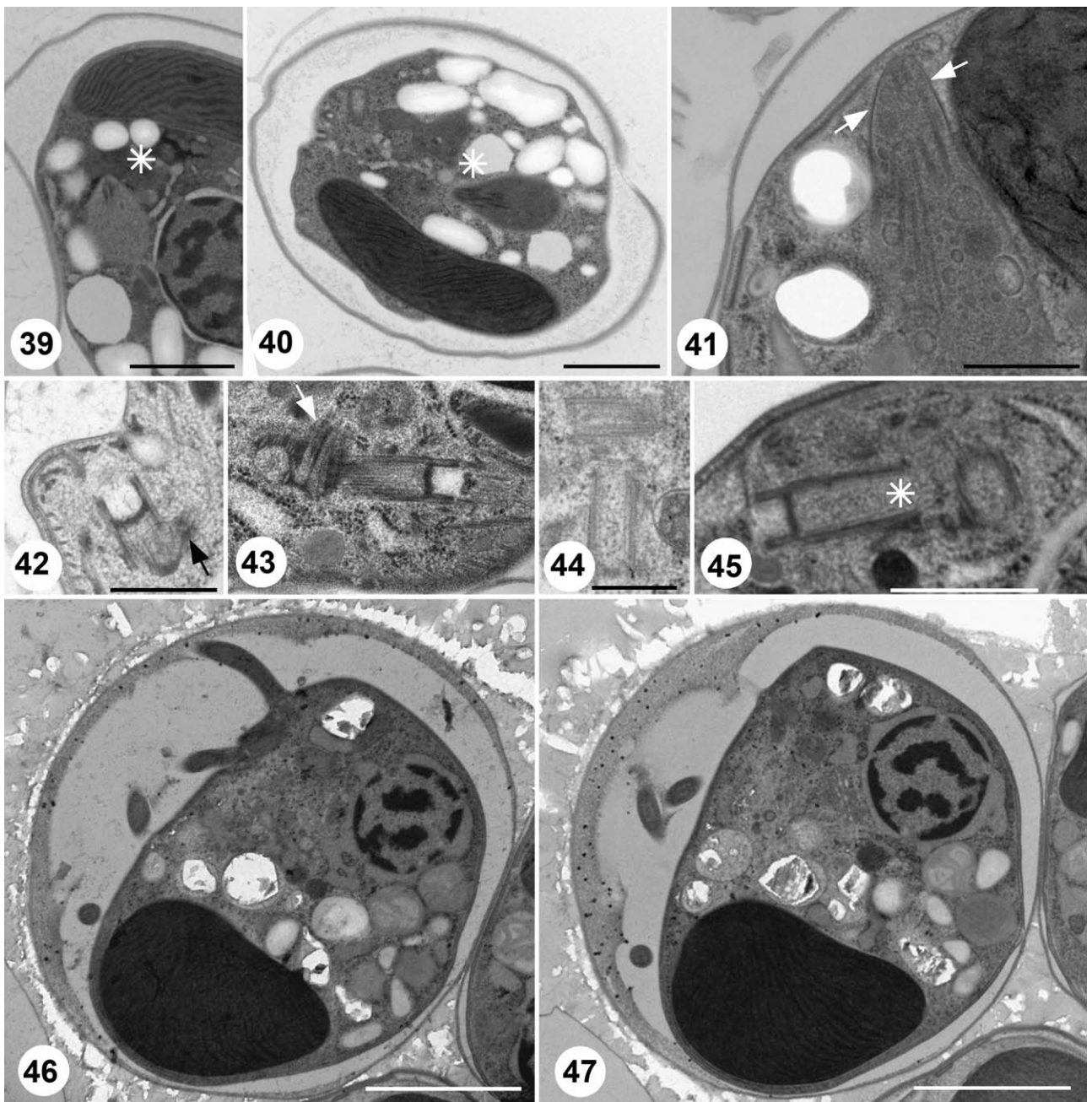
The earliest sign of the transformation into the flagellate stage that we observed may be the

appearance of a pack of microtubules in the anterior region of a pear-shaped cell (Fig. 28). Since this microtubular structure is composed of only several microtubules arranged in parallel, eventually forming an unlocked microtubular cone, we consider it to be homologous to the pseudoconoid of colpodellids and perkinsids. While this stage remains equipped with a complete corset of evenly spaced subpellicular microtubules located beneath the cortical alveoli (Figs 29 and 30), the emergence of a fully formed pseudoconoid is associated with the redistribution of the subplasmalemmal single-layered corset of microtubules apparent in Figure 31. Subsequently, the density of microtubules increases (Fig. 33), they undergo repositioning and some move into the cytosol (Figs 33 and 36).

The incomplete cone of about 20 longitudinal and likely interconnected microtubules is partly subtended by another layer of tubules directed in a different angle (Figs 35 and 36). The upper part of its mature form is cross-sectioned in Figure 38, while a tangential section of the differently tilted bi-layered part of the pseudoconoid is visible in Figure 36. Elsewhere in the cell, these parallel microtubules are arranged in a straight line (Fig. 35). They may represent a mature pseudoconoid that is cone-shaped only in its upper part, but opens downwards and thus verges into a straight line in its lower part. Alternatively, this line of tubules is just an early stage in the formation of the pseudoconoid.

Longitudinal sections of an early (Figs 39 and 40, asterisk) and more advanced pseudoconoid (Fig. 41, arrows) reveal the presence, in its lumen, of elongated electron-dense structures that are reminiscent of micronemes or rhoptries of the Apicomplexa (Figs 40 and 41). It is worth noting that during this transformation, the distance between neighboring alveoli increases (Fig. 41). The pseudoconoid is always formed in the vicinity of the basal bodies (Fig. 32), and this region of the cell is also characterized by the presence of a micropore associated with an interruption in the layer of alveoli (Fig. 35). Some longitudinal sections of micropores revealed small electron-dense regions adjacent to the pore (Fig. 37). Clathrin-coated vesicles (Fig. 35, arrow) are found in the vicinity of micropores (Fig. 35, asterisk).

A longitudinal section of the anterior part of the flagellum shows its basal body, the rather thick transverse plate, and the transition zone (Figs 42 and 43). A central doublet of microtubules is absent in the basal part of the flagellum (Fig. 32). Basal bodies of both flagella, mutually positioned at an angle of approximately 90° to each other (Fig. 44), are connected by an inconspicuous pluri-lamellar



Figures 39-47. Transmission electron microscopy. **Fig. 39.** A section containing a very small pseudoconoid (asterisk) that we consider the earliest stage. **Fig. 40.** A coccoid with a large plastid and numerous amylopectin granules that also contains a drop-shaped early pseudoconoid (asterisk). **Fig. 41.** Detail of a mature pseudoconoid revealing its peripheral location and subtle electron-dense tubules or fibres and vesicles present in its lumen. **Fig. 42.** Cross-sectioned basal body of a flagellum, close to the plasmalemma. Note the lamellar connector at the basis of the flagellum (arrow). **Fig. 43.** Longitudinal section through the long basal body and the transition zone. Lamellar connector (arrow) is positioned between both flagella. **Fig. 44.** The 90° angle between the basal bodies of forming flagella. **Fig. 45.** Peripheral location of the longitudinally and tangentially sectioned basal bodies of both flagella. Note the unusual length of the basal body (asterisk) and prominent transversal plate. **Fig. 46.** Coccoid at the stage of transformation into the flagellate. Note that the flagella have already been formed and ejected from the cell, which is still enclosed by the coccoid wall. **Fig. 47.** Another section of the same cell as in Figure 46. No paraflagellar rod is apparent in the cross-sectioned flagellum. Scale bar = 2 µm (46, 47), 1 µm (39, 40), and 500 nm (42-45).

connector (Fig. 43, arrow). Sections where one flagellum is sectioned longitudinally (Fig. 45, asterisk) and the other one is sectioned tangentially (Fig. 45) were also observed. The emergence of flagella in a coccoid cell undergoing transition is seen in Figures 46 and 47. The coccoid cell is still enclosed by an intact envelope, yet both flagella have not only been already formed, but can be seen cross-sectioned multiple times in the space between the cell and its enclosing wall (Fig. 46). No paraflagellar rod can be distinguished in cross-sectioned flagella. The flagellate clearly retains a large peripherally located plastid, as well as various storage granules.

Stage with Chromerosome

During the initial ultrastructural description, a small round vesicle with homogenously electron transparent lumen was interpreted as the mitochondrion (fig. 1 in Moore et al. 2008). However, a more detailed investigation showed that this assignment is incorrect and that this vesicle may be an early developmental stage of a novel structure described below. Following its enlargement (Fig. 48), the vesicle transforms into a bipolar shape. The only structure visible in its otherwise evenly electron transparent content is a bundle of fibre-shaped structures that stretch from one pole to the other (Fig. 48). In some sections it seems that these fibres are formed from an electron dense inclusion located next to the polar region of the vesicle (Fig. 49). While the prevalent shape of this structure is an elongated vesicle with prominently bipolar structure and fibres emerging from both poles (Figs 48, 49 and 51), rarely a constricted vesicle with somewhat disordered electron-dense fibres can also be found (Fig. 50). Each fiber measures 18 to 20 nm in diameter and is composed of a central electron-dense layer and peripheral electron-lucent layers. The highly regular distance between individual fibres is ~ 35 nm. In some micrographs, small yet prominent sacs with electron-dense periphery and core surround the vesicle (Fig. 51). Fine structural analysis at high magnification of the cross-banded fibres revealed their striped character (Fig. 52). Moreover, a double-layered membrane enclosing the vesicle can be discerned (Fig. 52).

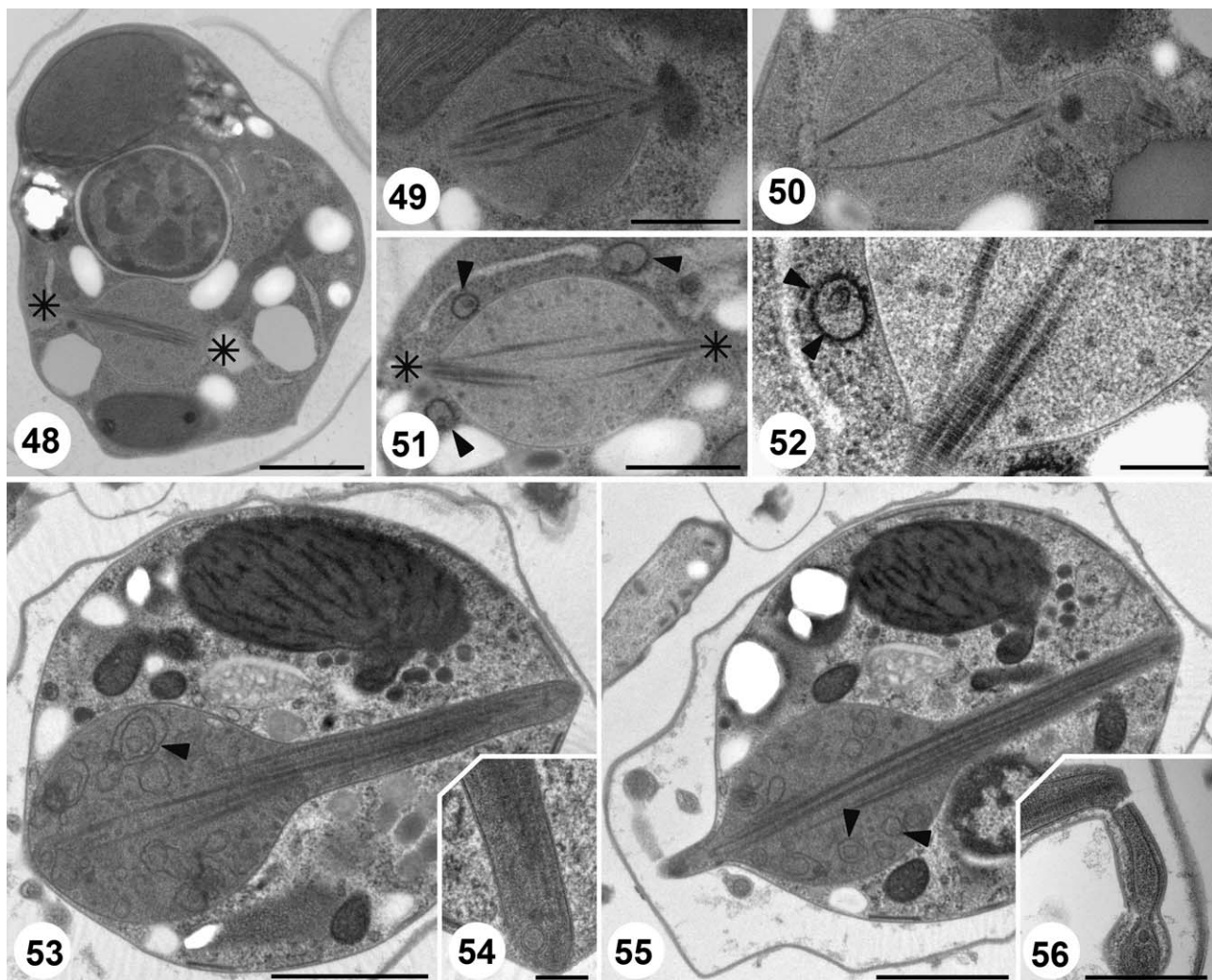
Further increase in the volume of this interesting cellular component leads to the formation of a highly characteristic shape that dominates the cell's ultrastructure and for which a designation "chromerosome" is proposed. Its etymology is derived from the combination of "Chromera" and "ejectosome", a tube-like organelle of cryptomonads

that bears resemblance with this cellular structure. In its anterior part chromerosome becomes enlarged, but in about 2/5 of its length, it abruptly narrows into a rod-like projection of consistent thickness. As part of the increased volume, the fibres grow while retaining their bundled arrangement (Fig. 53). At this stage the extended part of the chromerosome also contains multiple small membranous vesicles, some of which are enclosed by multiple concentric layers and appear to have the same content as their surrounding (Fig. 53, arrowheads). The identity of this extraordinary cell as a developmental stage in the cycle of *C. velia* is quite unequivocal, as the mitochondrion, plastid, micropyle, granules, cortical alveoli and surrounding membranes are highly reminiscent of the other stages. It appears though that due to enlargement of the cell, the individual alveoli become outstretched with the consequence of increased space among them (Figs 53 and 55). Even high magnification of the pointed tip of the pole-shaped protrusion did not disclose any ultrastructural features other than a tiny bi-layered vesicle (Fig. 54). What we consider the most advanced stage is shown in Figure 55, in which the chromerosome forms a finger-shaped protrusion, with the cell thus becoming polarized. Banded protrusion can be discerned in Figs 53 and 55. While the stripped fibres extend into the posterior part of the protrusion, no other morphological features are associated with it. In their mature form, the chromerosome resembles to some extent giant extrusomes or trichocysts of colpodellids and dinoflagellates. Unfortunately, only a very low number of cells present in the sectioned material contained the advanced form of chromerosome.

Discussion

Given the interest in *Chromera* and what it can tell us about the evolution of alveolates (Archibald 2009; Keeling 2008, 2009; Oborník et al. 2009; Janouškovec et al. 2010), a greater knowledge of its fine structure and life cycle are important. Here we undertook an analysis of *C. velia* culture using light and electron microscopy. In keeping with its phylogenetic position at the root of the apicomplexan lineage (Moore et al. 2008; Janouškovec et al. 2010), *C. velia* is, at the ultrastructural level, a unique mixture of characters so far described in apicomplexans, colpodellids, dinoflagellates and related groups (Table 1).

Under standard cultivation conditions, *C. velia* exists most of the time in the form of an oval



Figures 48-56. Transmission electron microscopy. **Fig. 48.** Section of a large coccoid containing a putative early stage of the chromerosome, which acquired a bipolar shape and contains a bundle of fibres stretched between two poles (asterisks). **Fig. 49.** A vesicle with fibres attached to (emerging from?) an electron-dense aggregate associated with its pole. **Fig. 50.** An early stage with somewhat disordered fibres that reach outside of the vesicle. **Fig. 51.** Two bundles of fibres that have attained a spindle-like shape, stretching outside into the polar regions. Note the presence of characteristic vesicles on its periphery (arrowheads), which are composed of an electron-transparent lumen and electron-dense core and outskirts. **Fig. 52.** Detail of the polar region revealing the evenly-spaced striped structure of the fibres. Note a high magnification of the accompanying vesicle with a clathrin-type form of peripheral projections (arrowheads). **Fig. 53.** A massively increased volume of the chromerosome, which at this advanced stage developed a prominent rod-like projection that stretches throughout the cell. The bulbous part contains numerous multimembranous vesicles (arrowhead), whereas the rod is filled with very long striped fibres. **Fig. 54.** A detail of the tip of the rod. Note the presence of a small bilayered vesicle in its very tip. **Fig. 55.** Longitudinally sectioned chromerosome with a prominent proboscis appearing from its extended region. Note that the cortical alveoli are not anymore of equal size and even distribution. They appear to be rather dilated due to increase in the cell volume. Multimembraned vesicles are labeled with arrowheads. Note multiple cross-sections of the twisted proboscis. **Fig. 56.** A serial section of cell in Figure 55, cutting through the extrusion. Scale bar = 1 µm (48, 53, 55), 500 nm (49-51, 56), and 200 nm (52, 54).

	tubular mitochondrial cristae	cortical alveoli	subpellicular microtubules	heterodynamic flagella	microtubular roots	plastid	conoid	pseudoconoid	micronemes	rhoptries (rhoptria-like)	micropyle	chromerosome	trichocyst
<i>Chromera velia</i>	+	+	+	+	+	-	-	-	-	-	-	-	-
dinoflagellates	+	+	+	+	+	-	-	-	-	-	-	-	-
colpodellids	-	-	-	-	-	-	-	-	-	-	-	-	-
perkinsiids	-	-	-	-	-	-	-	-	-	-	-	-	-
Apicomplexa	-	-	-	-	-	-	-	-	-	-	-	-	-

Table 1. Distinct morphological features of main groups of alveolates. “+” means presence of a character, “–” means its absence, “(+)” means its presence only in a subset of species, “?” contradictory or unknown.

cyst containing four coccoid cells that occasionally transform into highly motile bi-flagellated cells, which in turn revert to coccoid cells after a few hours. We speculate that the cyst-like cell inhabits corals while the function of the flagellate is to spread to other parts of the coral reef or eventually invade new corals (although whether *Chromera* lives within corals has yet to be demonstrated directly). Another possibility, proposed on the basis of observations in the culture is that the flagellates aid in escaping high light exposure.

The most conspicuous feature of the cell that appears to be unique to *Chromera* is the chromerosome. Originally, it was considered to be a mitochondrion (fig. 1a in Moore et al. 2008) but our detailed analysis shows that it resembles a novel extrusome-like structure. In a small proportion of cells, this enlarges and develops to form a prominent snout-like projection that eventually protrudes outside of the cell. The function of chromerosome remains totally obscure. There are no similar structures in apicomplexans, and the morphologically diverse extrusomes of dinoflagellates differ substantially from the chromerosome (Hausmann and Hülsmann 1996; Hoppenrath and Leander 2007; Leander and Hoppenrath 2008). At this point we can only speculate that it plays some role in the penetration of corals. It is also potentially associated with hunting of the algal or bacterial prey, since many algae within the chromalveolates are mixotrophs, and this could also explain the ability of *Chromera* to survive in the absence of light (Figs 57–62).

Several less conspicuous ultrastructural features also appear to be unique for *C. velia*, such as the finger-like projection on the short flagellum or the small but prominent wedge that might represent the cyst residuum. While the longitudinal ridges on the upper face of the coccoid wall are reminiscent of either tabulation characteristic for virtually all dinoflagellates (Hansen et al. 2007; Moestrup et al. 2008) or cytokinetic division ridges, the important difference is that in *Chromera* their arrangement does not seem to be reflected in the distribution of underlying alveoli or amphiesmal vesicles.

Remaining features found in individual stages of *C. velia* are not unprecedented, as they are shared with either apicomplexans, dinoflagellates or colpodellids (Table 1). As discussed earlier (Archibald 2009; Keeling 2008, 2009; Moore et al. 2008; Oborník et al. 2009; this work), thylakoids are arranged in stacks of three in plastids of both *C. velia* and dinoflagellates. Similarly, the ultrastructure of the *C. velia* micropore is virtually identical to that of apicomplexans (Hausmann

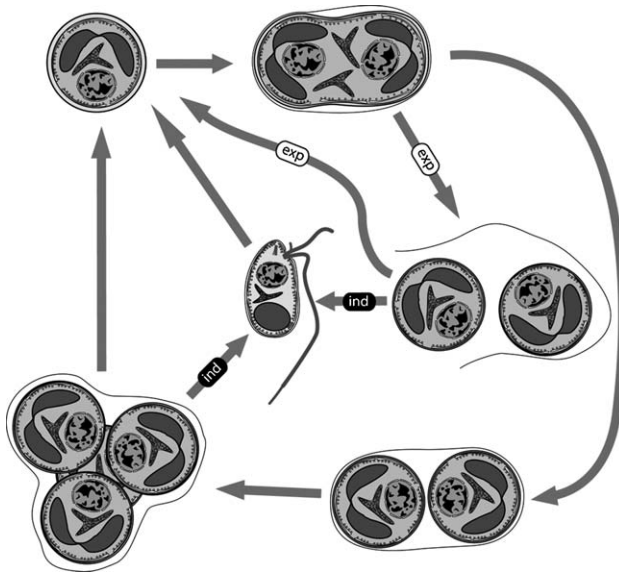


Figure 57. The life cycle of *C. velia*, reconstructed from stages observed under culture conditions. Exp – parts of the life cycle that appear to be upregulated in exponentially growing culture; Ind - parts of the life cycle that appear to be upregulated by light.

and Hülsmann 1996; Mehlhorn et al. 2009). The hallmark feature of all alveolates, the cortical alveoli, are prominently present in *C. velia*, although their distribution varies between different developmental stages: in coccoid cells flat alveoli are

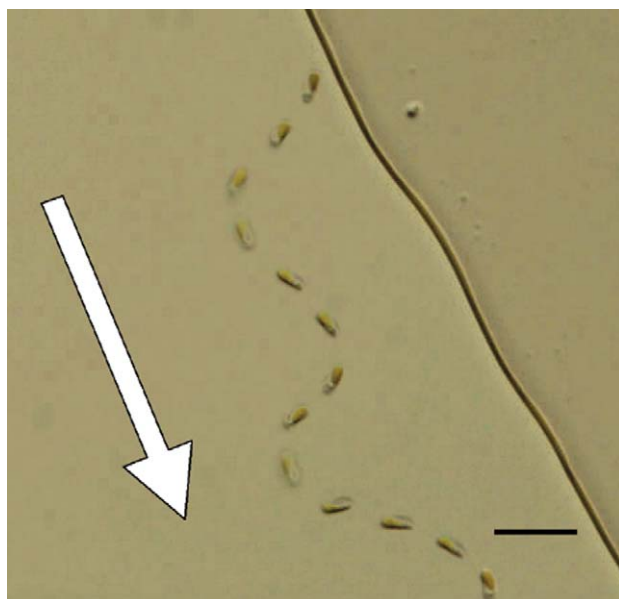


Figure 58. Snap-shots (each 125 ms) of swimming bi-flagellated cell, revealing its zig-zag movement. Scale bar = 20 μm .

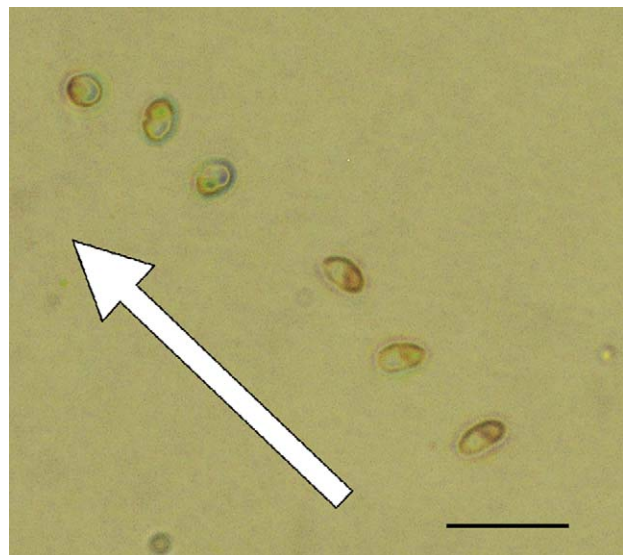
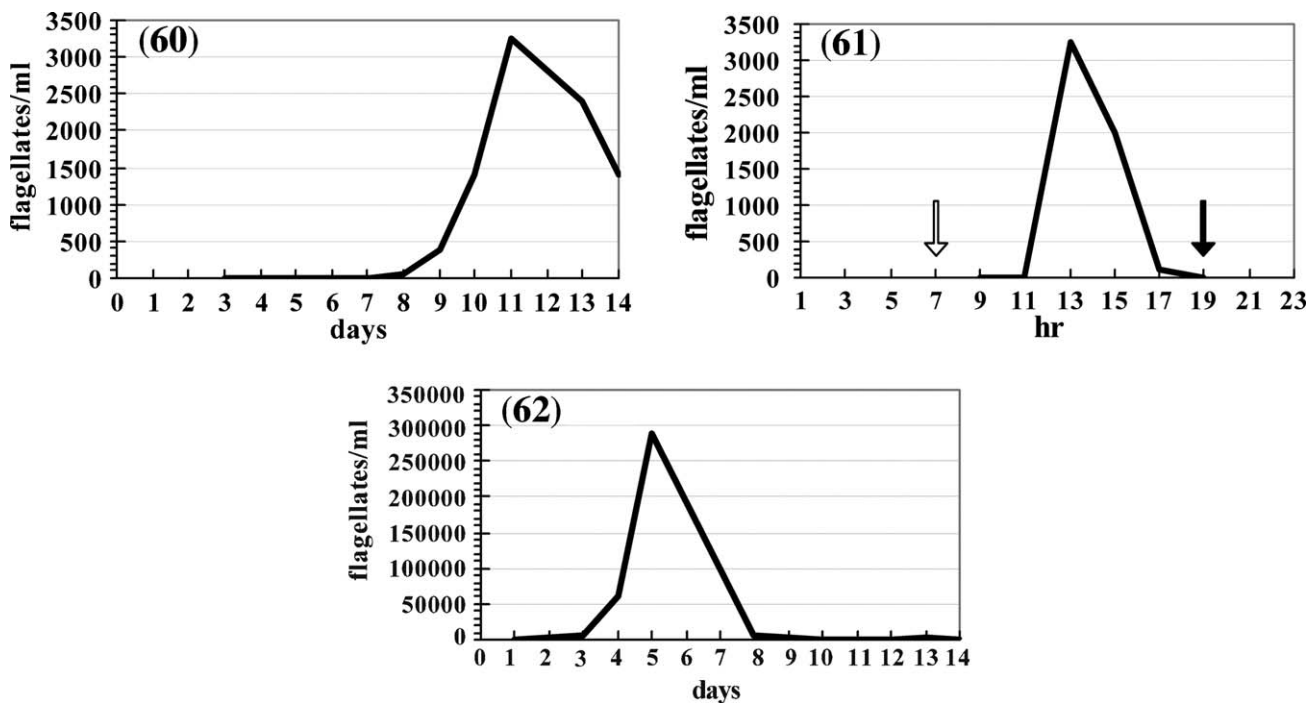


Figure 59. A sequence of figures of a single motile flagellate transforming into an oval cyst. Figures were taken each in an interval of 2 min. Scale bar = 20 μm .

regularly spaced and underlain by a microtubular corset but the distribution of these microtubules may signal transformation into the flagellate, in which they are distributed unevenly. This is at variance with most apicomplexans, which have a complete corset of the microtubules attached to the polar rings (Brugerolle 2002a; Morrisette and Sibley 2002). The non-uniform distribution is, however, reminiscent of the related *Perkinsus*, where gaps between densely adjoining microtubules have been described (Azevedo 1989). In most dinoflagellates chromosomes remain condensed throughout the life cycle (Kevin et al. 1969), and DNA is packed using unique histone-like proteins (Hackett et al. 2004; Rizzo 2003). In contrast, *C. velia* (like apicomplexans) possesses a nucleus with typical eukaryotic morphology, which is consistent with the presence of typical histones in its genome (Oborník et al. 2009).

Particular attention should be given to the structure considered by us to be a pseudoconoid. Perkinsids and colpodellids contain homologous structures, yet those seem to be somewhat more sophisticated (Azevedo et al. 1990; Brugerolle 2002a; Gestal et al. 2006). The fan-like pseudoconoid of *C. velia* seems to be assembled during the transformation of the coccoid cell into the flagellate, although this has to be confirmed by a more detailed analysis. The heterodynamic character of the *C. velia* flagella, mutual position of their basal bodies and a thinning of the long flagellum are also known from dinoflagellates and



Figures 60–62. Dynamics of flagellates under different culture conditions. **Fig. 60.** The appearance of flagellates in culture during a two-week long cultivation under standard conditions. The *y* and *x* axis show the number of flagellates/ml and days, respectively. **Fig. 61.** The appearance of flagellates in culture followed every other hour during day 11 (see previous graph). White and black arrows indicate the beginning and end of the light phase, respectively. The *y* and *x* axis show the number of flagellates/ml and hours, respectively. **Fig. 62.** The accelerated and amplified appearance of flagellates in culture illuminated with 11-fold higher light intensity. The *y* and *x* axis show the number of flagellates/ml and days, respectively.

colpodellids (Hansen et al. 2007; Moestrup et al. 2008). We were able to detect lamellar connectors between basal bodies of both flagella, yet they are substantially less prominent than those found in *Colpodella* (Brugerolle 2002a), *Cryptophagus* (Brugerolle 2002b) and especially dinoflagellates (Hansen et al. 2007; Moestrup et al. 2008).

One feature of the flagella of *C. velia* is particularly telling. Since the genome of *Plasmodium falciparum* uniquely lacks a set of genes needed for intraflagellar transport, it has to build its flagella in a different way (Briggs et al. 2004). Specifically, the flagellum is formed within the cytoplasm, and only then ejected (Killick-Kendrick and Peters 1978). The extended basal body of *C. velia*, without docking at the plasmalemma, is highly reminiscent of that of *Plasmodium*. Moreover, our observations strongly indicate that both flagella are assembled within the cytoplasm and, once they are fully formed, the internalized flagella are ejected. This appears to happen in the relatively short period between the rotation of the globular non-motile

cyst and the actual release of the flagellate. If *C. velia* is confirmed to lack flagellar transport and to eject fully formed flagella, this will be a very strong synapomorphy between the apicomplexans and chromerids.

We conclude that the flagellum of *C. velia* is not supported by a paraflagellar rod. While this rare feature is present in dinoflagellates and colpodellids (Brugerolle 2002a; Lukeš et al. 2009; Moestrup et al. 2008), it seems to be lacking in perkinsids and is certainly absent in apicomplexans (Hausmann and Hülsmann 1996; Steinhagen et al. 1990).

Concluding Remarks

The discovery of a photosynthetic coral symbiont closely related to the apicomplexans is an exciting development from the perspective of evolution of the parasitism in the apicomplexans. One could now imagine a relatively simple scenario where photosynthesis was lost in such a symbiont, leaving

it trapped within its host so that a heterotrophic life style, in the form of parasitism, was the only way to survive. Overall, it seems likely that photosynthesis was lost independently in apicomplexans and some colpodellids. In the colpodellids the loss of photosynthesis leads to a slightly different outcome, namely predation. However, a common denominator of the acquisition of nutrition by colpodellids and apicomplexans is the penetration of the prey or host cell, respectively, allowing them to either enter the cell or suck out its contents. The differences between these heterotrophic life styles are actually not very significant, the main difference being the size of their prey/host.

All in all, the light and electron microscopic study confirmed the status of *C. velia* as being an evolutionary link between apicomplexans and dinoflagellates. The combination of features shared with these phylogenetically related protist groups, as well as the presence of unprecedented structures such as the chromerosome, all support the need for further studies on this tiny alga of great potential importance from both the evolutionary and environmental perspective.

Methods

Cultivation conditions: The culture used in this study, strain CCMP2878, was obtained from the Culture Collection of Marine Phytoplankton (Boothbay Harbor, Maine). Cultivation occurred in the f/2 medium in seawater with a 12/12 light/dark regime at 26 °C. Occasionally, a 8/16 light/dark regime was also used. All experiments in which the (dis)appearance of flagellates in culture was studied were performed in triplicate. Regular light intensity was 3.15 W m⁻², accelerated exflagellation was induced by 35.8 W m⁻².

Light and electron microscopy: Both cysts and flagellates were examined by light microscopy with an Olympus IX70 microscope, and the measurements of cells were made with an image analyzer Camedia 5060 equipped with Quick PhotoPro 2.0. For scanning electron microscopy, cultured cells were fixed by the addition of 25% glutaraldehyde to the f/2 medium to final concentration 2.5% and incubated overnight at 4 °C. Next, pelleted cells were rinsed three times in filtered f/2 medium and immobilized by spreading onto a poly-L-lysine coated glass slide. Samples were then post-fixed in 2% OsO₄ and dehydrated in graded series of acetone, with 5 min incubation at each step. After drying by the critical point method (CPD2, Pelco TM), glass slides were mounted on an aluminum stub using

carbon conductive tape and a silver paste. Specimens were gold coated (SEM Coating Unit E 5100, Polaron) and observed in a field emission scanning electron microscope (JEOL JSM 7401-F).

For transmission electron microscopy, cultured cells were pelleted by centrifugation (15,000 rpm/5 min) and the compact pellet was transferred to gold-plated flat specimen carrier (thickness 0.5 mm, thick diameter 1.2 mm, depth 200 µm; Leica), frozen using a high pressure freezer (EM Pact, Leica) and transferred onto the surface of a substitution medium cooled by liquid nitrogen. Next, the temperature of the medium was quickly increased to -90 °C. The freeze substitution medium contained 2% OsO₄ in 100% acetone. Freeze substitution was performed using the AFS device (Leica) at -90 °C for 96 hrs and continued at -20 °C for additional 24 hrs. The rate at which the temperature was raised was 4 °C/1 hr and the substitution was finished when temperature reached 4 °C. Cells were transferred to room temperature, rinsed three times in 100% acetone and infiltrated in acetone/resin Polybed 812 (SPI) media. During infiltration, the specimen tubes were placed in a container containing 1 l of water and rotationally irradiated with a microwave (80W for 1 min) three times. The resin was allowed to polymerize at 60 °C for 2 days. Flat specimen carriers were removed after polymerization. Thin sections were cut using ultramicrotome (UCT, Leica), stained with uranyl acetate and lead citrate, carbon coated and observed in the transmission electron microscope (JEOL JEM 1010) equipped with MegaView III digital camera (SIS).

Acknowledgements

We thank Tom Cavalier-Smith and Catharina Gadelha (University of Oxford, Oxford), Alastair Simpson (Dalhousie University, Halifax) and David Roos (University of Pennsylvania, Philadelphia) for their valuable comments on the ultrastructure, and Ondřej Prášil (Institute of Microbiology, Třeboň) for help with cultivation. This work was supported by the Grant Agency of the Czech Academy of Sciences (IAA601410907) to M.O., the Ministry of Education of the Czech Republic (LC07032, 2B06129 and 6007665801) and the Praemium Academiae award to J.L., and the Canadian Institutes for Health Research (MOP-42517) to P.J.K. P.J.K. and J.L. are Fellows of the Canadian Institute for Advanced Research and P.J.K. is a Senior Scholar of the Michael Smith Foundation for Health Research.

References

- Archibald JM** (2009) The puzzle of plastid evolution. *Curr Biol* **19**:R81–R88
- Azevedo C** (1989) Fine structure of *Perkinsus atlanticus* n. sp. (Apicomplexa, Perkinsea) parasite of the clam *Ruditapes decussatus* from Portugal. *J Parasitol* **75**:627–635
- Azevedo C, Corral L, Cachola R** (1990) Fine structure of zoosporulation in *Perkinsus atlanticus*. *Parasitology* **100**:351–358
- Blank RJ** (1987) Cell architecture of the dinoflagellate *Symbiodinium* sp. inhabiting the Hawaiian stony coral *Montipora verrucosa*. *Marine Biol* **94**:143–155
- Briggs LJ, Davidje JA, Wickstead B, Ginger ML, Gull K** (2004) More than one way to build a flagellum: comparative genomics of parasitic protozoa. *Curr Biol* **14**:R611–R612
- Brugerolle G** (2002a) *Colpodella vorax*: ultrastructure, predation, life-cycle, mitosis, and phylogenetic relationships. *Eur J Protistol* **38**:113–125
- Brugerolle G** (2002b) *Cryptophagus subtilis*: a new parasite of cryptophytes affiliated with the Perkinszoa lineage. *Eur J Protistol* **37**:379–390
- Gestal C, Novoa B, Posada D, Figueras A, Azevedo C** (2006) *Perkinsoidea chabelardi* n.gen., a protozoan parasite with an intermediate evolutionary position: possible cause of the decrease of sardine fisheries? *Environ Microbiol* **8**: 1105–1114
- Hackett JD, Anderson DM, Erdner DL, Bhattacharya D** (2004) Dinoflagellates: a remarkable evolutionary experiment. *Am J Bot* **91**:1523–1534
- Hansen G, Botes L, De Salas M** (2007) Ultrastructure and large subunit rDNA sequences of *Lepidodinium viride* reveal a close relationship to *Lepidodinium chlorophorum* comb. nov. (= *Gymnodinium chlorophorum*). *Phycol Res* **55**: 25–41
- Hausmann K, Hülsmann N** (1996) Protozoology. Georg Thieme Verlag, Stuttgart
- Hoppenrath M, Leander BS** (2007) Morphology and phylogeny of the pseudocolonial dinoflagellates *Polykrikos lebourae* and *Polykrikos herdmaniae* n. sp. *Protist* **158**: 209–227
- Janouškovec J, Horák A, Oborník M, Lukeš J, Keeling PJ** (2010) A common red-algal origin of the apicomplexan, dinoflagellate and heterokont plastids. *Proc Natl Acad Sci USA* **107**:10949–10954
- Keeling PJ** (2008) Bridge over troublesome plastids. *Nature* **451**:896–897
- Keeling PJ** (2009) Chromalveolates and the evolution of plastids by secondary endosymbiosis. *J Eukaryot Microbiol* **56**: 1–8
- Kevin JM, Hall TW, McLaughlin JJA, Zahl PA** (1969) *Symbiodinium microadriaticum* Freudenthal, a revised taxonomic description, ultrastructure. *J Phycol* **5**:341–350
- Killick-Kendrick R, Peters W** (1978) Rodent malaria. Academic Press, London
- Köhler S, Delwiche CF, Denny PW, Tilney LG, Webster P, Wilson RJM, Palmer JD, Roos DS** (1997) A plastid of probable green algal origin in apicomplexan parasites. *Science* **275**:1485–1489
- Leander BS, Hoppenrath M** (2008) Ultrastructure of a novel tube-forming, intracellular parasite of dinoflagellates: *Parvilucifera prorocentri* sp. nov. (Alveolata, Myzozoa). *Eur J Protistol* **44**:55–70
- Lukeš J, Leander BS, Keeling PJ** (2009) Cascades of convergent evolution: The corresponding evolutionary histories of euglenozoans and dinoflagellates. *Proc Natl Acad Sci USA* **106**:9963–9970
- McFadden GI, Reith ME, Munholland J, Lang-Unnasch N** (1996) Plastid in human parasites. *Nature* **381**:482
- Mehlhorn H, Klimpel S, Schein E, Heydorn AO, Al-Quraishy S, Selmaier J** (2009) Another African disease in Central Europe: Besnoitiosis of cattle. I. Light and electron microscopical study. *Parasitol Res* **104**:861–868
- Moestrup Ø, Hansen G, Daugbjerg N** (2008) Studies on woloszynskiod dinoflagellates III: on the ultrastructure and phylogeny of *Borghiella dodgei* gen. et sp. nov., a cold-water species from Lake Tovel, N. Italy, and on *B. tenuissima* comb. nov. (syn *Woloszynskia tenuissima*). *Phycologia* **47**:54–78
- Moore RB, Oborník M, Janouškovec J, Chrudimský T, Vančová M, Green DH, Wright SW, Davies NW, Bolch CJS, Heimann K, Šlapeta J, Hoegh-Guldberg O, Longsdon Jr JM, Carter DA** (2008) A photosynthetic alveolate closely related to apicomplexan parasites. *Nature* **451**:959–963
- Morrisette NS, Sibley LD** (2002) Cytoskeleton of apicomplexan parasites. *Microbiol Mol Biol Rev* **66**:21–38
- Muller-Parker G, Davy SK** (2001) Temperate and tropical algal-sea anemone symbioses. *Invert Biol* **120**:104–123
- Oborník M, Janouškovec J, Chrudimský T, Lukeš J** (2009) Evolution of the apicoplast and its hosts: from heterotrophy to autotrophy and back again. *Int J Parasitol* **39**:1–12
- Rizzo PJ** (2003) Those amazing dinoflagellate chromosomes. *Cell Res* **13**:215–217
- Stat M, Carter D, Hoegh-Guldberg O** (2006) The evolutionary history of *Symbiodinium* and scleractinian hosts – Symbiosis, diversity, and the effect of climate change. *Persp Plant Ecol Evol Syst* **8**:23–43
- Steinhagen D, Lukeš J, Körting W** (1990) Ultrastructural observations on gamogonic stages of *Goussia subepithelialis* (Apicomplexa, Coccidia) from common carp *Cyprinus carpio*. *Dis aquat Org* **9**:31–36